AIAA AVIATION Forum
13-17 June 2016, Washington, D.C.
34th AIAA Applied Aerodynamics Conference

Revisiting the Transonic Similarity Rule: Critical Mach Number Prediction Using Potential Flow Solutions

Jeffrey J. Kirkman[1] and Timothy T. Takahashi[2]
Arizona State University, Tempe, AZ, 85287-6106

This paper revisits Von Kármán's Transonic Similarity Rule as explained by Schlichting. This rule postulates that an equivalent incompressible geometry corresponds to any given subcritical, high speed aerodynamic shape. We utilize panel method as well as Navier-Stokes CFD tools to better understand the actual behavior of wings in wing sections in high speed flight. We provide evidence that the classical "stretching" explanations given by famous authors are mutually inconsistent with one another. We also show that for many, but not all cases, a better physical analogy has the engineer visualize the Transonic Similarity Rule as a non-linear transformation of the effective velocity or dynamic pressure. We also discovered notable discrepancies in the Critical Pressure Coefficient equation given by famous authors.

Nomenclature

α	=	Angle of attack (deg)
β	=	Prandtl-Glauert Scaling Parameter
a	=	Speed of Sound
AR	=	Aspect Ratio (wing tip-to-tip span divided by mean geometric chord)
b	=	Wing Span
c	=	Wing Chord
CL	=	Lift Coefficient
CDi	=	Drag Coefficient
Cp	=	pressure coefficient
Cp^*	=	Critical Pressure Coefficient (associated with the onset of locally sonic flow)
M_∞	=	Freestream Mach number
Mcr	=	Critical Mach Number (associated with the onset of locally sonic flow)

[1] M.S. Candidate Aerospace and Mechanical Engineering, School for Engineering of Matter, Transport & Energy, P.O. Box 876106, Tempe, AZ. Student Member AIAA.
[2] Professor of Practice, Aerospace and Mechanical Engineering, School for Engineering of Matter, Transport & Energy, P.O. Box 876106, Tempe, AZ. Associate Fellow AIAA.

I. Introduction

TRADITIONALLY designed transonic wings employ various techniques to meet drag divergence criteria, including the spanwise distribution of camber, incidence, and thickness. Because shock induced flow separation dramatically increases overall drag, wing designers take great care to control the formation of shock waves.

One approach to delaying the onset of the shock formation is the use of leading edge sweep. However, work presented in the 2104 AIAA AVIATION conference, Takahashi, Dulin & Kady[1] found inconsistencies with Busemann's Simple Sweep Theory[2,3] as applied to a sheared wing. In a continuation of this work, presented in 2015 AIAA AVIATION conference, Takahashi & Kamat employed modern CFD to revisit the inconsistencies.[4] They found evidence that the published methods to predicting the onset of shock waves were inadequate. The data provided from the CFD runs did not inspire confidence that the classical theoretical predictions were applicable to real world swept wings.

In this current work, we seek to document the perils of applying many published transonic relationships to the design problem specifically the Transonic Similarity Rule. This theory holds that, for sub-critical flows, the high speed flow around any arbitrary body may be represented an incompressible, low speed flow around a body with a transformed geometry. Over the years, many authors have described this effect in terms of a geometrical "stretching" phenomenon. In our work, it became clear to us that common explanations are logically inconsistent. We raise question as to whether the mathematics of the Transonic Similarity Rule really means that a high speed aircraft can be modelled as a "stretched geometry" in incompressible flow. We suspect, and document in this paper, evidence that shows that the Transonic Similarity Rule results in equivalent flows which appear to have a Mach number dependent scaled velocity element.

In order to determine the correct formula for the Critical Pressure Coefficient, and therefore predict the Mach number associated with incipient supersonic flow, we used a variety of computational tools including commercial CFD, public domain 3D vortex lattice, and web-based 2D airfoil codes. Although our end goal is to determine the corrections on sheared and/or swept wings, the current authors found many inconsistencies between various derivations of the Critical Pressure Coefficient (Cp^*) for unswept wings. This paper will explore the works of Hermann Schlichting,[5] Dietrich Küchemann,[6] Eastman Jacobs and Theodore Von Kármán[7] from a 2D perspective. In this work, we set forth to determine the correct derivation for the Critical Pressure Coefficient and found that various published derivations lead to very different answers; although they all imply the same general physical trends. The inconsistencies between the various formulas at the Mach numbers in which real aircraft fly at, are significant enough to explain at least some of the problems noted by Takahashi & Kamat.[4]

II. Prior Art

A. Transonic Similarity Rules

In his NACA Technical Memorandum, Prandtl addressed the flow of compressible fluids, and presented his famous transformation to compare an incompressible flow, to a compressible flow.[8] This work provided a conceptual path to design aircraft that operate in the transonic regime. It is also the basis of many general purpose potential flow aerodynamic flow solvers. Prandtl's key equation comes in found in equation 10 in the original manuscript (reproduced here as equation 1):

$$\frac{\delta u}{\delta x}\left(1-\frac{{u_0}^2}{a^2}\right)+\frac{\delta v}{\delta y}+\frac{\delta w}{\delta z}=0 \qquad (1)$$

This equation provides a freestream velocity dependent correction on the flow in the *x*-direction. This is proven to be a powerful equation and the only assumptions are that the velocities derived are small compared to the flow, u_0, and that the velocity in the *v* and *w* direction are small relative to the speed of sound, *a*. We do not dispute the utility of this equation, merely the physical explanation of its action.

Four possible physical explanations can arise from this equation (see Figure 1). All invoke the famous, Prandtl-Glauert scaling parameter:

$$\beta = \sqrt{1 - \frac{u_0^2}{c^2}} = \sqrt{1 - M_\infty{}^2} \qquad (2)$$

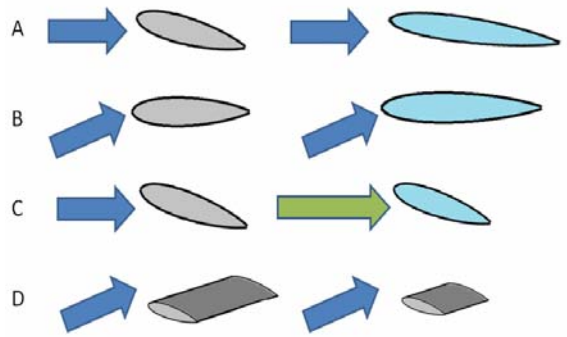

Figure 1 – Possible Geometry Implications of the Prandtl-Glauert potential flow equation

One interpretation (represented by Figure 1A) says that the scaling term acts upon the *x* axis dimension of the geometry terms, in other words, P-G scales the longitudinal geometry in the axis of on-coming flow by a factor proportional to the reciprocal of β, $1/\sqrt{1 - M_\infty{}^2}$. Here, the inflow velocity is exactly aligned with the *x* axis; thus a wing at angle-of-incidence must be represented by an inclined geometry. Thus, the *x* axis stretching results in the equivalent incompressible shape being longer in the *x*, or chordwise direction but no longer in the *y*, or thickness direction. Such a transformation implies that the equivalent incompressible shape has greater effective area, a lower effective thickness-to-chord ratio (*t/c*), and a lower incidence (α) than the actual high-speed shape.

A second possible interpretation (represented by Figure 1B) says that the scaling term acts upon the *x* axis dimension of the geometry terms, in other words, P-G scales the longitudinal geometry in the axis of on-coming flow by a factor proportional to the reciprocal of *β*, $1/\sqrt{1 - M_\infty{}^2}$. In this view, the geometry is exactly aligned with the *x* axis; but the inflow velocities comprise a steady flow in both the *x* and *y* directions; *u* and *v* are non-zero. Thus, the *x* axis stretching results in the equivalent incompressible shape being longer in the *x*, or chordwise direction but no longer in the *y*, or thickness direction. Such a transformation implies that the equivalent incompressible shape has greater effective, a lower effective thickness-to-chord ratio (*t/c*), and the same incidence (α) than the actual high-speed shape.

The third interpretation (represented by Figure 1C) says that the scaling term acts upon the *u* dimension of the flow terms, in other words, P-G scales the effective flow speed by a factor proportional to β; simply $\sqrt{1 - M_\infty{}^2}$. In this view, the inflow perfectly aligns itself with the *x* axis. The geometry is inclined to represent incidence; however, no Mach number dependent "stretching" takes place. A velocity scaling viewpoint has the equivalent incompressible shape maintain the same area, incidence and thickness-to-chord ratio as the actual high-speed shape. However, the scaled effective velocity means that the actual pressure coefficients (along with lifting forces, pressure drag forces and pitching moments) increase in a manner proportional to $1/\sqrt{1 - M_\infty{}^2}$.

The final interpretation (represented by Figure 1D) says that the scaling term acts upon the *y* axis dimension of the geometry terms, in other words, P-G scales the transverse geometry in the axis of on-coming flow by a factor proportional to *β*., $\sqrt{1 - M_\infty{}^2}$. Thus, the *y* axis stretching results in the equivalent incompressible shape being shorter in the *y*, or spanwise direction but no longer in the *x*, chordwise or, *z*, thickness direction. Such a transformation implies that the equivalent incompressible shape has the same incidence and thickness-to-chord ratio (*t/c*) as the actual high-speed shape, but a smaller area and lower aspect ratio.

Prandtl[8] solves the modified form of this equation, an elliptic equation for subsonic velocities and hyperbolic for supersonic velocities, to explain the geometric transformation implied by high-speed, compressible (but subcritical) flows. Prandtl states that in order for a contour in a compressible fluid to maintain the same result as in an incompressible fluid, the "contour must be made thinner" and likewise, the angle of attack must decrease. This is, in essence interpretation 1A as stated above.

It is interesting to note that Prandtl describes this work as being a geometrical change. He of course talks about comparing a compressible solution back to an incompressible one. Other authors view it in reverse; taking an incompressible solution and correcting it to a compressible one. His primary discussion is how it relates to a contour thickness as well as an angle of attack change, yet it appears to be an attempt to make sense of the work he laid out with only a slight comment on the correction factor being related to the velocities themselves. Prandtl "hand waves" the discussion to relate a mathematical model to some form of a physical relationship.

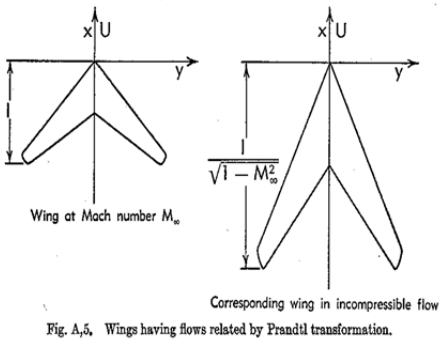

Fig. A,5, Wings having flows related by Prandtl transformation.

Figure 2 - Jones & Cohen explanation of Prandtl-Glauert Stretching.[12]

Although less famous than Prandtl, Göthert made considerable contributions to the theory of three-dimensional flows at high subsonic speeds. In NACA TM-1105 from 1946, Göthert discussed the effects of "stretching" and incompressible solution in order to obtain the compressible flow solution.[9] Reproduced below is Göthert's version of the potential flow equation:

$$\frac{\partial^2\phi_c}{\partial x_c^2}+\frac{\partial^2\phi_c}{(\sqrt{1-\mathrm{M}\infty^2}\times\partial y_c)^2}+\frac{\partial^2\phi_c}{(\sqrt{1-\mathrm{M}\infty^2}\times\partial z_c)^2}=0 \qquad (3)$$

Göthert claims that the streamlines of a compressible flow are distortions of the streamlines of the incompressible by a "Prandtl Factor" of $1/\sqrt{1-M_\infty{}^2}$, but in the *y* and *z* directions (as opposed to a reciprocal transformation in the *x* direction). Göthert argues that the compressible flow is comparable to the incompressible flow by a decrease in the *y* and *z* contours. Therefore, his "stretching" of the incompressible profile is actually a contraction along the *y* and *z* coordinates (the *x* coordinate is defined in the free stream direction).

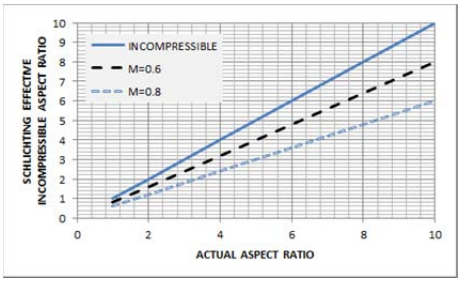

Figure 3 – Schlichting / Jones & Cohen explanation of Prandtl-Glauert Stretching. – effects on AR

R.T Jones approached Prandtl's transformation in NACA TR-863,[10] as well as his later writings in Jones & Cohen's *High Speed Wing Theory*.[11] These works explain the transformation in two dimensions as a stretching in the *x*-direction by the factor of $1/\sqrt{1-M_\infty^2}$, therefore it is the chord of the airfoil that the stretching is applied to. This explanation is purely geometrical and only occurs in the *x*-direction. Jones & Cohen go on to argue the transformation in relation to a three-dimensional wing as well.[11]

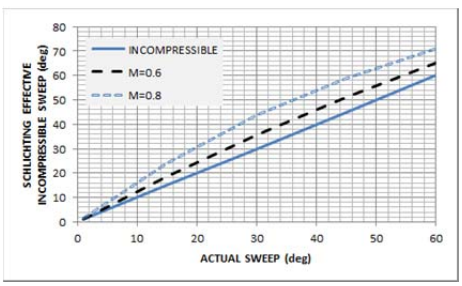

Figure 4 – Schlichting / Jones & Cohen explanation of Prandtl-Glauert Stretching. – effects on sweep

According to Jones & Cohen,[11] the compressible flow relationships that govern a two-dimensional wing sections apply broadly to three-dimensional wings (see Figure 2). They state that, geometrically, the longitudinal stretching means that the equivalent area increases while the span remains the same. Thus both the effective sweep angle and the aspect ratio of the equivalent incompressible wing will vary due to the "stretching" in the chord. They hold that the aspect ratio of a compressible wing is comparable to a smaller aspect ratio wing in incompressible flow. Thus the effective incompressible area increases by the Prandtl-Glauert factor, $1/\sqrt{1-M_\infty^2}$, while the effective incompressible aspect ratio declines by a factor of $\sqrt{1-M_\infty^2}$. Jones does not expressly differentiate between the Figure 1A and Figure 1B physical analogies in either work.[10,11] Because he does not discuss angle-of-attack effects directly, either explanation could fit his reasoning.

Hermann Schlichting also approaches the "stretching" transformation as a similarity rule.[5] Unlike Prandtl,[8] he transforms the wing at compressible flow speeds into an equivalent incompressible wing by transforming the *y* coordinate; he does not discuss the *z* coordinate in his transformations. Mathematically it is algebraic rearrangement of terms first shown by Prandtl[8] that follows the method proposed by Göthert.[9]

Schlichting holds that the following geometrical transformations apply to compare a wing in compressible flow to an equivalent wing in incompressible flow. First, he applies a "stretching" on in the spanwise, *y*, direction:

$$x_{inc} = x \tag{4a}$$
$$y_{inc} = y \cdot \sqrt{1 - M_\infty{}^2} \tag{4b}$$
$$z_{inc} = z \tag{4c}$$

Thus, he implies the following properties of a transformed wing: that the span, *b*, scales downwards with increasing Mach number but the chord remains constant.

$$b_{inc} = b \cdot \sqrt{1 - M_\infty{}^2} \tag{5a}$$
$$c_{inc} = c \tag{5b}$$

This means that the aspect ratio, *AR*, declines with increasing Mach number, while the taper ratio, *TR*, thickness-to-chord ratio, *t/c*, and effective angle of attack, α, all remain constant:

$$AR_{inc} = AR \cdot \sqrt{1 - M_\infty{}^2} \tag{6}$$
$$TR_{inc} = TR \tag{7}$$
$$\left(\frac{t}{c}\right)_{inc} = \left(\frac{t}{c}\right) \tag{8}$$
$$\alpha_{inc} = \alpha \tag{9}$$

Similar to Jones & Cohen,[11] Schlichting[5] indicates that the effective sweep of the incompressible wing increases with increasing Mach number although for different reasons (stretching in the spanwise as opposed to chordwise direction):

$$\cot(\varphi_{inc}) = \cot(\varphi) \cdot \sqrt{1 - M_\infty{}^2} \tag{10}$$

The effects of these transformations may be seen in Figures 3, 4 and 5. Figure 3 plots equation (6) and finds, at higher Mach numbers, that the equivalent incompressible wing has a lower Aspect Ratio than the physical wing. Figure 4 demonstrates how equation (10) affects the effective sweep. As the Mach number increases, Schlichting's rule finds that swept wings behave as if they were incompressible wings of greater sweep (and smaller span).

Figure 5 shows the geometric transformations described by Schlichting. Thus we may interpret this Figure to illustrate how a "given" physical wing can be represented by a series of "transformed" or equivalent incompressible wings. Because Schlichting holds that $y_{inc} = y \cdot \sqrt{1 - M_\infty{}^2}$, his equivalent incompressible wing is of a smaller wingspan (and area) than that of the physical wing in compressible flow. This is a key point where Jones and Schlichting differ. Jones[10,11] implies that an increase in Mach number leads to an equivalent incompressible wing of greater effective area. Schlichting[5] states that an increase in Mach number

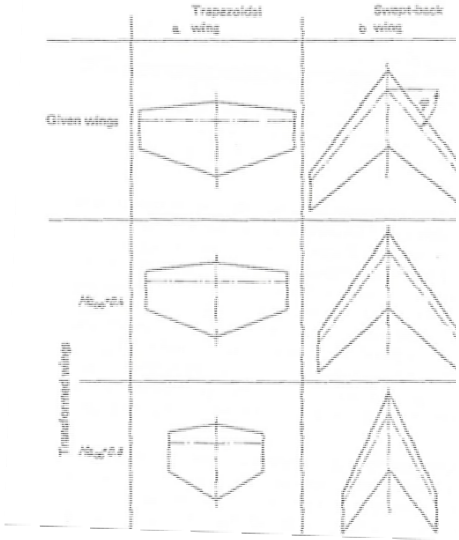

Figure 5 – Schlichting graphical explanation of the Transonic Similarity Rule.[5]

leads to an equivalent incompressible wing of lesser effective area. Clearly, both analogies cannot be correct!

Thus, this argument, presented by Schlichting, indicates that he basically follow the guidelines of Figure 1D; changes in Mach number impact the effective span and area of the wing, but not the incidence or thickness.

In other areas, Schlichting's[5] transformations agree with the work of Jones & Cohen,[10,11] as they both argue an equivalent incompressible wing has a lower aspect ratio compared to the compressible wing. The difference occurs is how the incompressible solution is "stretched". Schlichting states that the stretching occurs along the *y*-axis, therefore changing the aspect ratio, the span, and even changing an equivalent sweep angle. However, one major point that Schlichting states is: for the unchanged profile (airfoil) between incompressible and compressible flow, the angle of attack will be the same.

This is an interesting point that Schlichting continues to point out in his derivations of the transformation of the lift coefficient, pressure coefficient, and moment coefficient of the incompressible wing to those of the compressible wing. He does not give an explanation as to the reason for this, but he also does not consider a *z*-direction transformation in any of his work. Schlichting only concerns himself with the *x*-*y* plane in his transformations.

Schlichting also holds the following transformation formulas to hold for an "inclined wing of finite span in subsonic flow" where $\alpha = \alpha_{inc}$ where the geometry at incompressible speeds is otherwise identical to that at compressible speeds:

$$Cp = \frac{1}{\sqrt{1-M_\infty{}^2}} \cdot Cp_{inc} \tag{11}$$

$$CL = \frac{1}{\sqrt{1-M_\infty{}^2}} \cdot CL_{inc} \tag{12}$$

$$\frac{dCL}{d\alpha} = \frac{1}{\sqrt{1-M_\infty{}^2}} \cdot \left(\frac{dCL}{d\alpha}\right)_{inc} \tag{13}$$

$$\alpha_0 = \alpha_{0_{inc}}: \tag{14}$$

$$Cm = \frac{1}{\sqrt{1-M_\infty{}^2}} \cdot Cm_{inc} \tag{15}$$

$$CD_i = \frac{1}{\sqrt{1-M_\infty{}^2}} \cdot CD_{i_{inc}} \tag{16}$$

That is, the pressure coefficients at high speeds increase inversely proportional to the Prandtl-Glauert scaling parameter, β; the lift coefficient at any given angle-of-attack increase inversely proportional to β; the slope of the lift coefficient with respect to angle-of-attack increases inversely proportional to β; the zero-lift-angle of attack remains unchanged, and the induced drag coefficient increases inversely proportional to β. It therefore follows that the inviscid aerodynamic efficiency at a given angle of attack, *CL/CDi* should not change as a function of Mach number because both the lift and induced drag coefficient scale directly with the reciprocal of β. To our eye, Schlichting's arguments are inconsistent with those shown earlier in his book; they more closely follow the transformation implied by Figure 1C.

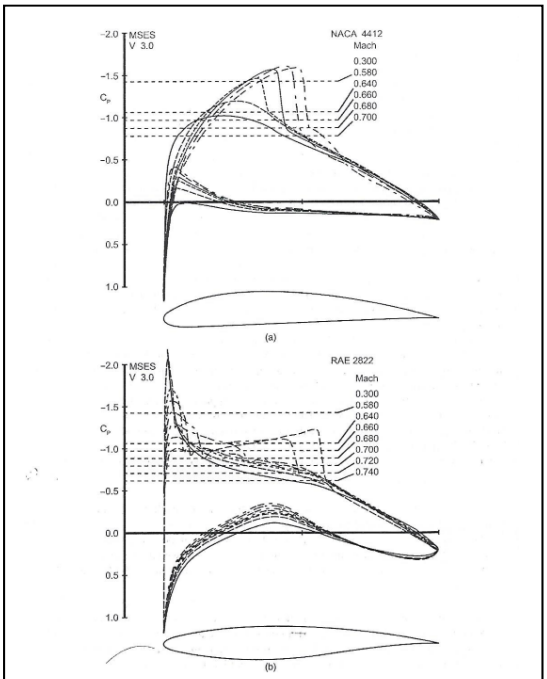

Figure 6 – Description of relationship between Shock Wave Formation and *Cp** from McLean.[12]

The work done by Doug McLean in his book *Understanding Aerodynamics*[12] very briefly covers "stretching" as Jones and

Prandtl would call it. McLean states that the pressure disturbances produced by an airfoil will maintain the general characteristics, however they will gradually increase. He does not call this a "stretching", but instead just points out the increase in the pressure distribution in a compressible flow, compared to an incompressible flow.

Figure 6 from Mclean,[12] shows the effect of the Mach number on the pressure distributions. The airfoil remains at a constant angle of attack, however the pressure distributions appear as though the airfoil is "thicker" as the Mach number increases. This is the perfect example to McLean's discussion on the change in the pressure coefficient in compressible flow. These arguments also seem to imply the existence of an effective dynamic pressure transformation, more than any formal geometric morphing. Thus, McLean circumstantially implied flow that behaves along the lines of Figure 1C.

Mark Drela's work in *Flight Vehicle Aerodynamics* explains the Prandtl-Glauert Transformation in a modified form.[13] Drela defines the scaling factor as $\beta \equiv \sqrt{1 - M_\infty^2}$ and uses this β to define the geometrical transformations, but instead of Prandtl's transformation in the *x*-direction, or Schlichting's transformation in the spanwise, y, direction, he applies transformations in both the y and z-directions.

Drela[13] applies these transformations are applied to the *y* and *z*-directions, because Drela performs the transformation of the compressible flow, back to the incompressible solution. Therefore, the argument is the *y* and *z* coordinates decrease in the incompressible flow, when compared to the compressible flow solution. The incompressible angle of attack is decreased as well as the aspect ratio has decreased. In the figure below, Drela shows the real flow transformed into a mathematically equivalent flow

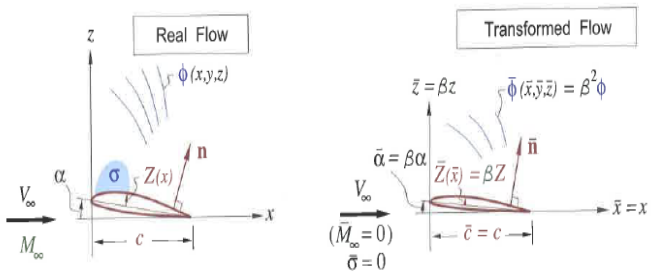

Figure 7- Transformed Equivalent Incompressible Geometry showing an increase in area and decrease in angle-of-attack. After Drela.[13]

Drela[13] sketches the geometric transformations in his writings, reproduced here in Figure 7. Drela shows that the real flow (compressible) can be transformed to an incompressible flow through a decrease in the angle of attack, a decrease in the *z*-direction (including airfoil thickness), and the *x*-direction remaining untouched.

Each author above has a different explanation on the stretching and how it applies to the equivalent incompressible geometry. While some agree with one another wholeheartedly, others have some issues with some of the work. Even when the authors cite another as the source of their "stretching", they come out as different interpretations! This starts to make one wonder, who is right on the transformation and what is the correct physical explanation? We will validate many of these proposed relationships using modern computation in Section IV of this paper.

B. Critical Pressure Coefficient

To properly design transonic wings, engineers must pay careful consideration to match the flight conditions where incipient shock wave occurs with the planned operating characteristics of the airplane. This is due to the large drag impact that a shock wave can produce when it induces flow separation. The point where a shock wave begins to form is Critical Mach Number of the wing, the Mach number in which sonic flow is first attained somewhere on the wing. Traditionally, we associate this phenomenon with the speed where the peak underpressure of the local airflow falls below the Critical Pressure Coefficient (Cp^*). We need to precisely capture the speed and lift coefficient where this occurs because the overall design of a wing hangs in the balance of being able to properly meet design performance targets in terms of lift and drags well as the necessary volume for structure, fuel and other components.

Theodore Von Kármán, in his famous paper on compressibility effects[7], uses Glauert's approximation[14] in order to derive his equation for the Critical Pressure Coefficient. Glauert's approximation allows the mathematician to

linearized the perturbation velocities under an argument that holds that while higher order perturbation terms exist, they are negligible. This leads Von Kármán, to derive his equation for the Critical Pressure Coefficient:

$$Cp^* = \frac{2\left[\left(1-M_\infty^2\right)^{3/2}\cdot\left(1+M_\infty^2\right)^{1/2}\right]}{M_\infty} \tag{17}$$

Kármán goes on to state that the equation above may not be exact due to the derivation from the linear theory. In order to improve upon this, he suggests that we consider Eastman Jacobs' derivation from the thermodynamic relationship is a good starting point:

$$Cp^* = \frac{2\left[1-\left(\frac{2+(\gamma-1)M_\infty^2}{\gamma+1}\right)^{\gamma/(\gamma-1)}\right]}{\gamma M_\infty^2} \tag{18}$$

Kármán points out that the derivation from Jacobs includes some necessary corrections to errors introduced by the linearized theory. Interestingly, we cannot find a direct source of this derivation on *scholar.google.com*. None of Eastman Jacobs' authored papers seem to explain his rationale. While Jacobs worked for the NACA, the Critical Mach Number lines in the famous NACA TR-824 airfoil guide[15] follow von Kármán's equation (17) to infer the Critical Mach Number from the peak recorded underpressure found during low speed testing.

John Anderson, in *Introduction to Flight*, approached the Critical Pressure Coefficient through thermodynamic relationships.[16] Anderson derives equation 19 by the definition of the pressure coefficient and the isentropic relationships between the static pressure and total pressure.

$$Cp^* = \frac{2}{\gamma M_\infty^2}\left\{\left[\frac{2+(\gamma-1)M_\infty^2}{\gamma+1}\right]^{\gamma/(\gamma-1)} - 1\right\} \tag{19}$$

Schlichting's[5] definition of the Critical Pressure Coefficient relies on the knowledge of the Critical Mach Number. Schlichting argues that if the Critical Mach Number is known, then the Critical Pressure Coefficient can be easily determined by the minimum pressure coefficient on the surface. He does make a correction to his equation as well into include the sweepback of the wing. Reproduced below is Schlichting's derivation for the Critical Pressure Coefficient on the wing:

$$Cp^* = -\frac{2}{\gamma+1}\frac{1-Ma_{\infty_{cr}}^2(\cos\varphi)^2}{Ma_{\infty_{cr}}^2} \tag{20a}$$

For simple two-dimensional flow, Schlichting's equation reduces to the following form:

$$Cp^* = -\frac{2}{\gamma+1}\frac{1-Ma_{\infty_{cr}}^2}{Ma_{\infty_{cr}}^2} \tag{20b}$$

This is a notably simpler equation than proposed by either von Kármán or Jacobs.

Küchemann[6] in his famous book, *The Aerodynamic Design of Aircraft*, describes the critical conditions through the use of isobars on a swept wing. He argues that on a swept wing the critical condition occurs where the flow normal to the isobars reaches the local speed of sound. Küchemann uses his swept wing example to derive through the thermodynamic relationships between pressure, velocity, and total head to reach the equation below.

$$Cp^* = \frac{2}{\gamma M_\infty^2}\left\{\left(\frac{2}{\gamma+1}\right)^{\frac{\gamma}{\gamma-1}}\left(1+\frac{\gamma-1}{2}M_\infty^2\,(\cos\varphi)^2\right)^{\frac{\gamma}{\gamma-1}} - 1\right\} \tag{21a}$$

Which, when simplified for simple two-dimensional flow, reduces to:

$$Cp^* = \frac{2}{\gamma M_\infty^2}\left\{\left(\frac{2}{\gamma+1}\right)^{\frac{\gamma}{\gamma-1}}\left(1+\frac{\gamma-1}{2}M_\infty^2\right)^{\frac{\gamma}{\gamma-1}}-1\right\} \qquad (21b)$$

Although argued from a different perspective, and algebraically distinctive, Küchemann's equation (21b) turns out to be numerically identical to the Eastman Jacobs equation (18) cited by Kármán.[7]

The Critical Pressure Coefficient is crucial in understanding the incipient shock wave formation on a wing in transonic flight. Although many of the authors above apply similar, if not identical basic governing physics, each author follows a personal path to arrive at fundamentally different final equations which supposedly estimate *Cp**. The inconsistencies between each derivation inspires no hope in the design process to accurately predict the shock wave formation.

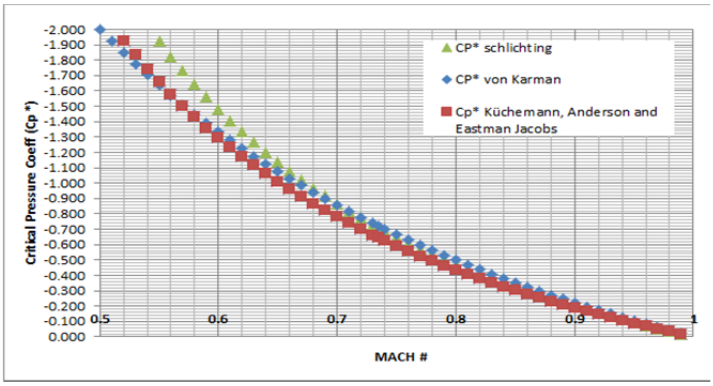

Figure 8- Comparison of *Cp** equations (Schlichting, von Kármán, Küchemann, E. Jacobs and Anderson. *Cp** as a function of Mach.

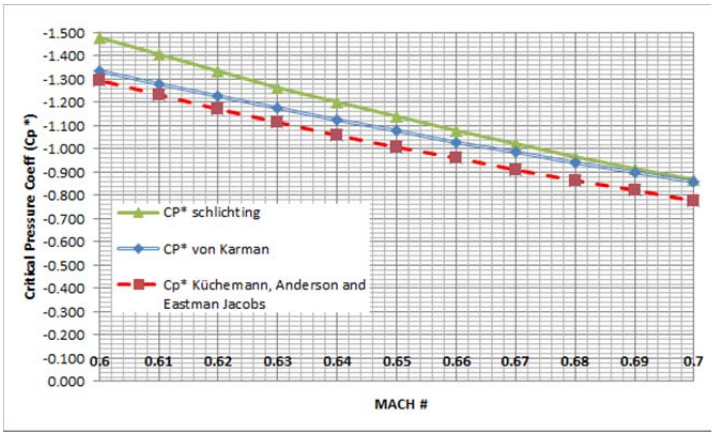

Figure 9- Detailed comparison of *Cp** equations (Schlichting, von Kármán, Küchemann, E. Jacobs and Anderson. *Cp** as a function of Mach at a typical airfoil design point.

We plot each famous equation (Schlichting (20b), von Kármán (17), Küchemann (21b), E. Jacobs (18) and Anderson (19)) together as Figure 8. Although the equations vary, they each maintain the basic physical constraints. For example, each equation approaches zero as the Mach number approaches one. Therefore, as the freestream flow approaches sonic velocity, the pressure coefficient relating to the sonic flow point is zero. When the free stream flows at Mach 1, any disturbance that leads to increased velocities and reduced pressures triggers a shock wave. It is also interesting to note that for two dimensional flow, Küchemann, Eastman Jacobs, and Anderson's Critical Pressure Coefficients are mathematically equivalent. This is expected since they are all derived through thermodynamic relationships.

Although these equations approach zero as the Mach number approaches 1, these equations differ significantly at lower Mach numbers. Since real aircraft wings must carry lift in flight, incipient shock formation typically occurs in the Mach 0.6 to 0.7 range (for swept wings, this is in terms of Mach number normal to the leading edge). Figure 9 shows the variation of the Critical Mach Number implied by the different formulas that occur in this range. A given pressure coefficient can imply a variation of Critical Mach Number as much as $\Delta M \sim 0.03$ in this region. It is enough of discrepancy to cause performance figures to not be met; if a wing section ostensibly designed for Mcr=0.66 actually has a Mcr=0.63, the speed corresponding to the onset of drag divergence will likely diminish proportionately.

It is this discrepancy that the current authors have set out to investigate further in **Section IV**.

III. Computational Methods Used in This Study

In this study, the current authors employed various aerodynamic codes as well as commercial CFD in order to perform the necessary computations These computations included running various wings and airfoils at various Mach numbers and angles of attack. The purpose was to gather data to clarify the mysterious phenomena of "stretching" and to determine the "most correct" equation for the Critical Pressure Coefficient.

VORLAX

VORLAX is a compressibility-corrected subsonic/supersonic potential flow solver developed by Lockheed-California (now Lockheed Martin) under contract from NASA.[17] The code allows the user to input geometry in three forms: 1) simple, thin flat panels, 2) thin, cambered panels, or 3) a thickness simulating "sandwich panels." *VORLAX* outputs a variety of flow solution data: 1) overall force and moment coefficients suitable to build an aerodynamic database (lift, drag, side force, pitching moment, rolling moment, and yawing moment), 2) surface panel net differential pressure coefficients (for thin flat and cambered panels), 3) surface panel actual pressure coefficients (for thickness simulated "sandwich panels), and 4) off-body wake survey velocity vectors. We used *VORLAX* to determine the correct forms of the various transformations proposed by Schlichting. We also use *VORLAX* alongside CFD to investigate Critical Mach Number predictive capabilities of the various equations. Because *VORLAX* is incapable of simulating a shock wave, we can identify regions of incipient sonic flow where the *VORLAX* solution diverges significantly from a CFD solution.

JAVAFOIL

JAVAFOIL is a simple program built upon a potential flow analysis and a boundary layer analysis. *JAVAFOIL* uses a higher order panel method to solve the potential flow equations and to obtain an inviscid flow velocity on the airfoil in question.[18] It also implements the criteria set forth by Eppler, to solve the boundary layer differential equations.[19]

JAVAFOIL does not handle supersonic velocities, and is able to handle mild transonic Mach numbers through the scaling of the basic potential flow solution through the Kármán-Tsien correction.[7] Although *JAVAFOIL* includes Critical Mach Number predictive capability; the documentation does not identify the specific equation used to infer either Cp^* or Mcr.

We used the *JAVAFOIL* applet to verify some of the CFD results in low speed conditions, as well as to compare the transonic solutions to the potential flow model.

ANSYS Fluent

ANSYS Fluent software solves the Navier-Stokes equations through either a density-based or pressure-based solver. Due to the analysis of airfoils being in the transonic regime, the density-based solver was used.

For the airfoil sections, we created a 2D C-grid, with the inlet and outlet placed a large distance from the airfoil, so that the boundaries did not interfere with the solution. A grid convergence was built on the base grid in order to verify the results of the computation.

IV. TRADE STUDIES TO IDENTIFY WHICH RELATIONSHIPS ARE EXACT VS APPROXIMATE

We set forth to determine the correct transformation of incompressible flow solutions into compressible solutions starting with the Mach number dependent relationships proposed by Schlichting's *Aerodynamics of the Airplane*.[5] These were given earlier in the paper as equations (6) through (16).

A. Prandtl-Glauert Effect on Pressure Distribution

The first transformation we set to examine was the transformation on the pressure distribution. According to Schlichting the compressible pressure distribution is related to the incompressible pressure by the inverse of the Prandtl-Glauert parameter: $Cp = 1/\sqrt{1 - M_\infty^2} \cdot Cp_{inc}$. (Equation 11 from above).

In Figure 10, we show the Mach number dependence of pressure coefficients as computed using a *VORLAX* sandwich panel model. Here, we model an aspect ratio 20 NACA 0006 section wing. We run *VORLAX* at three Mach numbers: 0.0, 0.6 and 0.8 and at a variety of angles-of-attack. From the converged solutions, we extract centerline pressure profiles. In each case, we compare the pressure coefficients predicted at high speed against an application of equation 10 to the pressure coefficients predicted at M∞=0 (pure incompressible). In Figure 10a, we show the effects of M∞=0.8 flow on the non-lifting wing. The Schlichting approximation matches the *VORLAX* computation closely, but not exactly. In Figure 10b, we show the effects of M∞=0.6 oncoming flow to the wing at incidence. Here, the Schlichting approximation matches the *VORLAX* computation extremely closely, but not exactly.

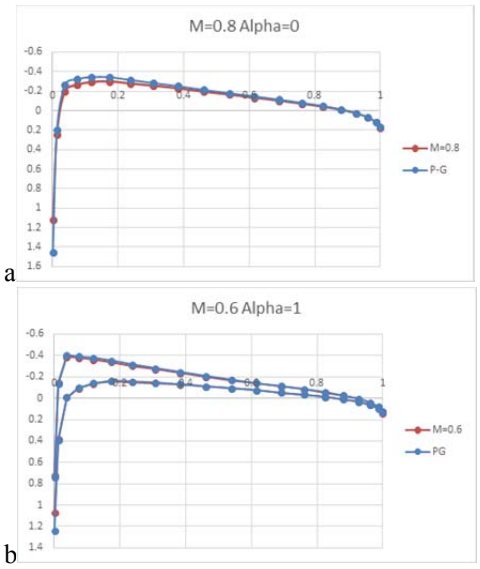

Figure 10 – VORLAX sandwich panel solutions. NACA 0006 section. VORLAX run at M∞=0.6, M∞=0.8. Prandtl-Glauert predictions based upon VORLAX solutions at M∞=0.0.

In the *ANSYS Fluent* 2-D inviscid compressible flow solution of a NACA 64-012 airfoil section, we find the Prandtl-Glauert correction is shown to be almost exact for the low transonic flows (around M∞=0.6) and a reasonable but imperfect approximation for flow at the higher Mach numbers. Here, we compared the high speed compressible flow solution compared with an M∞=0.1 solution as transformed by Equation 11. With the exception of the stagnation point at the leading edge, where Prandtl himself said the correction would be inconsistent,[8] the simplified correction provides a good estimation for the compressible solution.

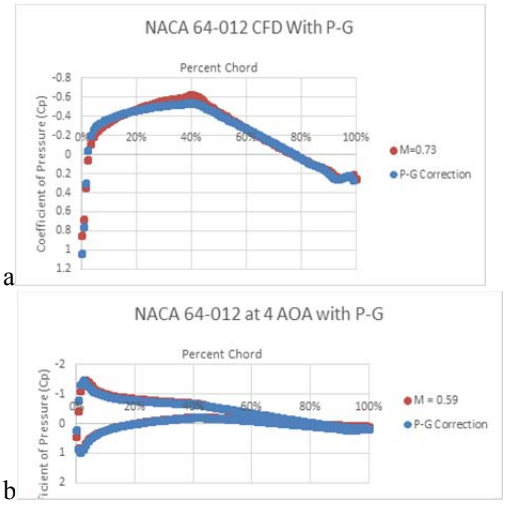

Figure 11 – ANSYS FLUENT 2D solutions. NACA 64-012 section. FLUENT run at M∞=0.59, M∞=0.73. Prandtl-Glauert predictions based upon FLUENT solutions at M∞=0.1.

Both *VORLAX* and *ANSYS Fluent* agree in many respects. Both solutions find that the induced pressures from thickness follow the Schlichting / Prandtl-Glauert rule; they are all stronger at high speeds than their incompressible equivalents (refer Figure 10a and Figure 11a). Thus, as air speed increases, the actual wing feels "thicker" than it does at low speeds. For the lifting cases (refer to Figure 10b and Figure 11b), we see that the induced pressures due to incidence, camber and thickness follow the

Prandtl-Glauert scaling rule. Thus, both upper and lower high-speed pressure coefficients are noticeably greater than those predicted in incompressible flow; as speed increases the actual wing feels "thicker" than it does at low speeds; it also feels "larger" than it does at low speeds. However, the shape of the incidence dependent pressure profile does not change as we would expect if there were an effective change in incidence due to "stretching."

From this evidence, we confirm Schlichting's transformation from Equation 11. At the same time, we refute "stretching" analogies 1A, 1B and 1D. To explain the noted effects, we believe that analogy 1C must be true; the "stretching" effect manifests itself as a non-linear transformation of magnitude of the incoming flow.

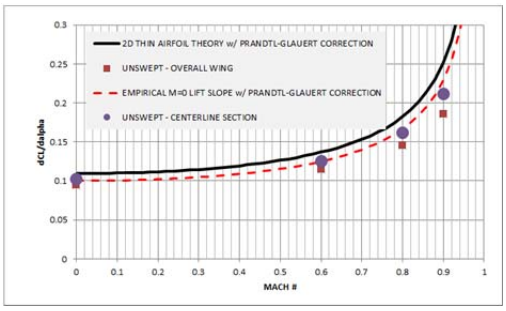

Figure 12 – VORLAX solutions. Flat plate AR=20 model. Prandtl-Glauert predictions based upon VORLAX solutions at M∞=0.0.

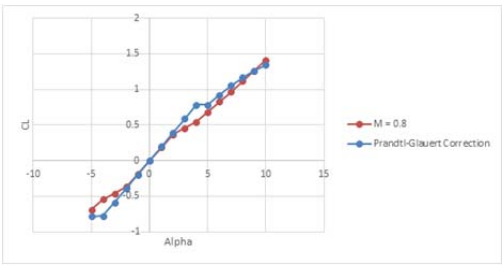

Figure 13 – *JAVAFOIL* solutions. NACA 64-012 2-D model. Prandtl-Glauert predictions based upon *JAVAFOIL* solutions at M∞=0.0.

B. Prandtl-Glauert Rule applied to 2D Lift Curve Slope

According to Schlichting transformations equations (12) and (13), both the lift and the lift curve slope will also contain a Prandtl-Glauert correction. Schlichting argues, since the pressure distribution experiences a transformation in compressible flows, and since the lift is direct integration of the pressures, the lift and lift curve slope will receive the same transformation: $\frac{\partial C_L}{\partial \alpha} = \frac{1}{\sqrt{1-M_\infty^2}} \frac{\partial C_L}{\partial \alpha}_{inc}$.

We see, in Figure 12, how well the lift curve slope of the *VORLAX* computed compressible solution is approximated by the Prandtl-Glauert correction. One distinction that is found in our finite wing data comes from the fact that neither the overall wing lift slope nor the centerline section lift slope of the AR=20 attains the theoretical 2D value. Thus, to make a fair assessment of Schlichting's transformation we must "pivot" our transformations about the incompressible (M∞=0) centerline lift coefficient found in the numerical solution. Following such a procedure, we find that Schlichting' s approximation is nearly exact for the low transonic speeds (around M∞=0.6) and slightly differs at higher transonic speeds.

Figure 13 above shows the lift curve results from *JAVAFOIL* for a NACA 64-012 airfoil. Here we ran the code at *M∞=0*, and transformed the solution using Schlichting's relationship and compared it against a solution found running this code at *M∞=0.8*. Because the solution of *JAVAFOIL* is not a pure inviscid solver, some inconsistencies form between the two solutions due to the Eppler boundary layer model used by this code. However, these results demonstrate that the Schlichting version of the Prandtl-Glauert correction factor on both lift and lift-slope is reasonable.

From this evidence, we confirm Schlichting's transformations predicted using Equations 12 and 13. At the same time, we refute "stretching" analogy 1A. Such a transformation would increase the effective area, but diminish the effective incidence of the wing. We see no such evidence here that analogy 1C is wrong; if we were to hold that the "stretching" effect manifests itself as a non-linear transformation of magnitude of the incoming flow, both the lift and lift-slope of the wing would scale in lockstep with the local pressure coefficients (as Figures 10, 11, 12 and 13 all demonstrate).

C. Schlichting' s rule for zero lift angle and pitching moment

Schlichting's Transonic Similarity rule includes a correction for the zero-lift angle of the compressible wing; $\alpha_0 = \alpha_{0_{inc}}$ (equation 14). His transformation states that the angle of attack for the compressible wing does not change, and includes that the zero lift angle of the wing should be the same as well.

Figure 14 shows the *VORLAX* solution of a thin cambered wing (NACA 23 camber form) at various Mach numbers and angles of attack with the moment reference point chosen at the wing quarter-chord area centroid. These results, plotting lift as a function of incidence, demonstrate shows that the zero lift angle of the wing does not vary with Mach number. Schlichting's transformation, or lack of transformation, appears to be correct regarding the zero lift angle.

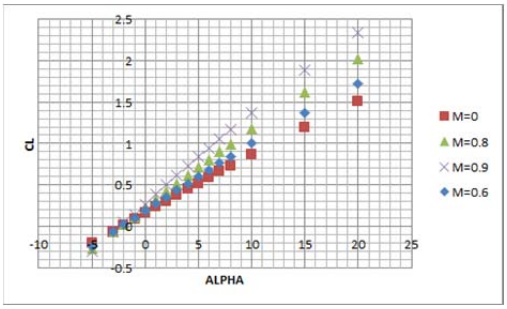

Figure 14 – VORLAX solutions. AR=6 thin cambered wing. NACA 23 camber form. Lift vs Angle of Attack.

From this evidence, we believe that *VORLAX* continues to substantiate the Figure 1C physical analogy. When the "stretching" effect manifests itself as a non-linear transformation of magnitude of the incoming flow held at a prescribed incidence with respect to the body.

Schlichting also states that the Transonic Similarity rule should apply the Prandtl-Glauert scaling term to the zero-lift pitching moment as well; that $Cm = \frac{1}{\sqrt{1-M_\infty{}^2}} \cdot Cm_{inc}$ (equation 15). In Figure 15, we plot the quarter-chord reference pitching moment coefficient against the lift coefficient. At a first glance the zero-lift pitching moment appears to follow the Prandtl-Glauert correction factor. Under close scrutiny, we realize that the proposed correction is dreadfully wrong. The computational results show a Mach dependent effect that decreases the aerodynamic stability of the wing (moving the aerodynamic center forwards) as the incoming flow increases in speed. Since we saw in Figures 12 and 14 that $dCL/d\alpha$ closely follows the Prandtl-Glauert scaling law, the change in the slope of *dCm/dCL* with Mach number implies that pitching moment cannot follow the same law. In Figure 16, we examine the high speed *VORLAX* solutions as opposed to incompressible results transformed by equation 15. Here we see a strong disagreement between the direct solution and Schlichting's transformation; Schlichting's method is clearly incorrect.

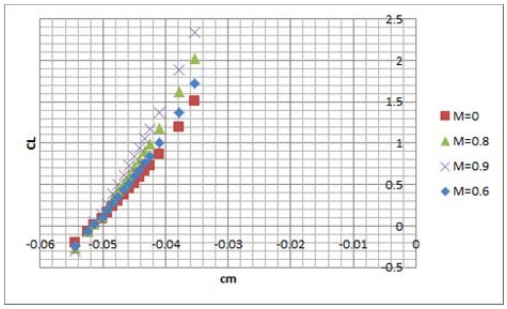

Figure 15 – VORLAX solutions. AR=6 thin cambered wing. NACA 23 camber form. Pitching Moment vs. Lift.

From this new evidence, we find a situation where *VORLAX* does not substantiate any proposed physical analogy. If the "stretching" effect manifests itself as a non-linear transformation of magnitude of the incoming flow held at a prescribed incidence with respect to the body, both lift and pitching moment would scale by the same effect and no change in stability would occur.

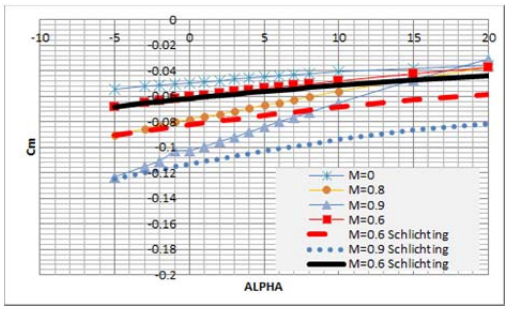

Figure 16 – VORLAX solutions. AR=6 thin cambered wing. NACA 23 camber form. Pitching Moment vs. Angle of Attack.

D. Schlichting's Rule for induced drag

Schlichting's transformation on the induced drag derives from the transformation on the lift as well as his purported spanwise scaling of the wing span; physical analogy 1D. Schlichting also claims that: $C_{Di} = \frac{1}{\sqrt{1-M_\infty^2}} C_{Di_{inc}}$ (equation 16); thus both Lift and Induced Drag scale in lockstep. We show how computation does not support the veracity of this relationship.

Figure 17 plots drag polars of an AR=6 flat-plate wing modelled with 100% analytical credit for leading edge suction. In Figure 17a, we examine an incompressible solution that builds a drag polar with $dCDi/dCL^2=0.555$; pure lifting line theory would predict $dCDi/dCL^2 = 1/(\pi\, AR) = 0.0530$. Thus, the untwisted wing has a theoretical efficiency of 96%. In Figure 17b, we compare the M∞=0 incompressible solution corrected to M∞=0.9 using equation 16 against the direct M∞=0.9 solution. We see that the correction quickly deviates from the *VORLAX* solution. Something is dreadfully wrong.

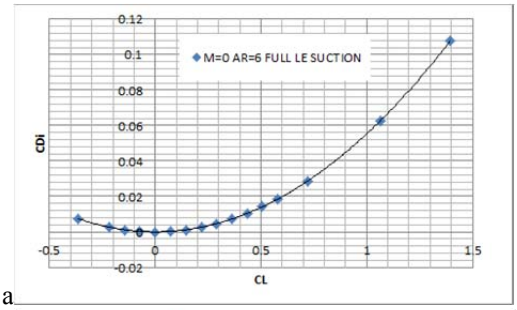

a

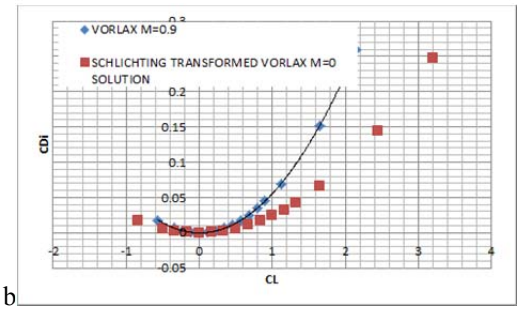

b

Figure 17 – VORLAX solutions. AR=6 thin flat plate wing with 100% credit for leading-edge suction.

Indeed, in Figure 18 we plot $dCDi/dCL^2(M)$ as derived from a series of fully converged *VORLAX* solutions. Although the slope of $dCL/d\alpha$ changes with Mach number, the value $dCDi/dCL^2$ remains remarkably constant. In order to match this data, we propose an alternative relationship:

$$C_{Di} = 1/(1 - M_\infty^2) \cdot C_{Di_{inc}} \qquad (22)$$

This is because *CDi* is predominately a function of CL^2; if *CL* follows a $\frac{1}{\sqrt{1-M_\infty^2}}$ relationship, CL^2 must follow a $\frac{1}{1-M_\infty^2}$ relationship.

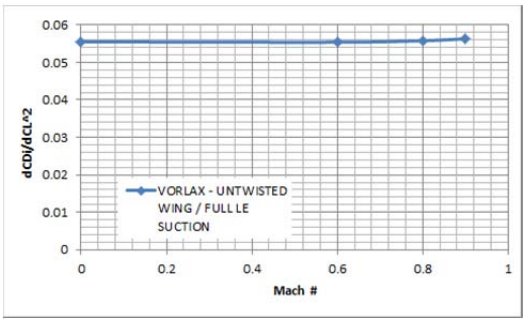

Figure 18 – VORLAX solutions. AR=6 thin flat plate wing with 100% credit for leading-edge suction.

From this evidence, we believe that *VORLAX* substantiates the Figure 1C physical analogy. When the "stretching" effect manifests itself as a non-linear transformation of magnitude of the incoming flow held at a prescribed incidence with respect to the body, lift increases proportionally to the square of enhanced velocity and drag increases proportionally to the square of the lift.

E. Critical Mach / Critical *CP**

As discussed in Section II of this paper, famous authors have derived a multitude of equations to estimate the Critical Pressure Coefficient (refer back to Figures 8 and 9). Because the equations diverge from one another at lower Mach numbers; where they predict higher critical underpressures (more negative values of *Cp**), we can "experimentally" and "computationally" determine which equations are clearly incorrect and which equations have positive predictive value.

For the transonic 3D wing design problem, wing sweep is employed to reduce the Mach number normal to the leading edge to approximately M∞~0.6. It is precisely in this region that the classic equations differentiate

themselves from one another. Since real wings carry lift and must contain structure, the designer is particularly interested in the interplay between underpressures created by lift generation (incidence and camber) and those created by thickness. For example, if an initial design relies upon an overly optimistic value of Cp^*, drag divergence will onset early. The aircraft designer will either be forced to live with reduced performance or will need to accept a schedule slip to redesign a thinner (potentially structurally unfavorable) wing.

Let us begin by examining wind tunnel pressure test data of a NACA 0012 section.[20] C. D. Harris tested two dimensional flow on a NACA 0012 section in the NASA/LaRC 8-foot transonic pressure tunnel. These tests were performed holding flow velocity constant and changing the Mach number by lowering the static temperature, hence lowering the speed of sound of the flow. The 2D airfoil section was positioned at varying angles of attack to gather upper and lower surface pressure data

In Figure 19, we examine experimental data collected at $M\infty=0.601$ for two different incidences ($\alpha=3.86^o$ and $\alpha=5.86^o$). The classic equations predict Cp^* to be: 1) Schlichting: $Cp^*=-1.474$, 2) Anderson: $Cp^*=-1.288$; 3) Jacobs: $Cp^*=-1.288$; 4) Küchemann: $Cp^*=-1.288$; 5) Von Kármán, $Cp^*= -1.328$. Here we see that while the equations do differ slightly from one another, the test data cannot differentiate between them. Experiment finds no major shock wave at $\alpha=3.86^o$ and a noticeable shock at $\alpha=5.86^o$. Among the analytical predictions, Schlichting's Cp^* equation predicts subcritical flow $\alpha=3.86^o$, while the others predict marginally supercritical flow at that condition. All five equations predict supercritical flow at $\alpha=5.86^o$. Thus, high quality published test data confirms the broad utility of all of the analytical estimation formulas but cannot differentiate between them.

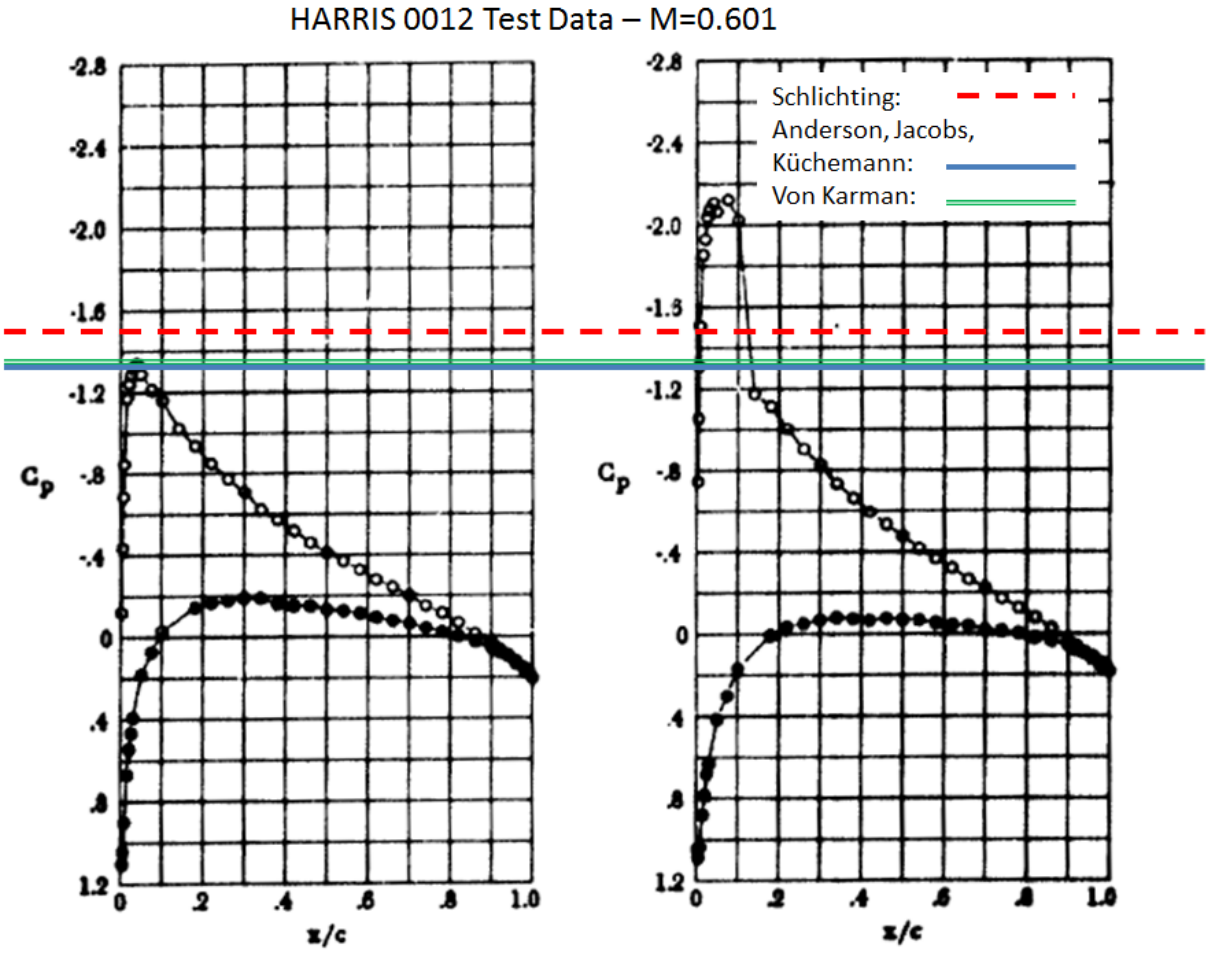

Figure 19 – Wind tunnel test data of a NACA 0012 Airfoil (2D) at $M\infty=0.601$.

In light of limited available test data, to use this basic procedure to find the best equation suitable to determine the Critical Mach Number, and therefore the Critical Pressure Coefficient, we turned to computation.

In this work, we began by modelling a symmetric NACA 64-012 airfoil in *ANSYS FLUENT*. We ran solutions varying Mach numbers at two angles of incidence: $\alpha=0^o$ and $\alpha=4^o$. We began with a low speed solution. We estimated the critical condition based upon the equations in Section II. We then ran a fine sweep of high speed solutions varying the Mach number in 0.01 increments around the predicted critical point to determine the actual conditions associated with the onset of locally supersonic flow.

Our process here was slow and methodical. It is crucial to take small increments in Mach number to truly capture the incipient shock formation. We also took into account the likelihood of shockless, supercritical flow developing right around the sonic point. Since the shock wave is sometimes difficult to track in the CFD solution, we took careful consideration to document the local Mach number of the near surface flow.

The initial testing on zero degrees angle of attack showed Küchemann, Anderson and Eastman Jacobs were correct in the prediction of the shock wave, occurring at $M\infty=0.73$. However, Schlichting and Kármán's equations were off by a few hundredths, therefore we set to carry lift on the airfoils in order to force the Critical Mach to occur at lower Mach numbers, where the difference is more noticeable.

Figure 20 plots computed upper and lower surface pressure coefficients of the NACA 64-012 airfoil at zero degrees angle of attack and $M\infty=0.73$. At $M\infty=0.73$ (Figure 20a), the shock-wave is in the early stages of forming at the minimum pressure point. The flow has just reached its Critical Mach Number (Figure 21), which was predicted by Eastman Jacobs, Anderson and Küchemann, but not by Schlichting or Von Kármán (Figure 20b). This data here gives compelling evidence that Schlichting and Von Kármán were incorrect in their predictions of the Critical Pressure Coefficient.

Figure 21 plots the Mach number of the $M\infty=0.73$ flow over the airfoil at zero degrees angle of attack. We show in this figure that the local Mach number is exceeding one. Although the flow does not visually appear to form a shock wave, the airfoil has clearly reached its critical condition. As shown with the pressure coefficient plots

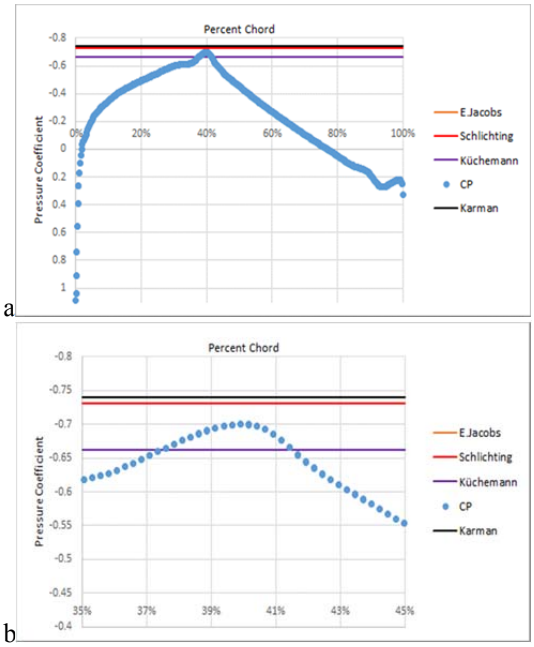

Figure 20 – ANSYS/Fluent computation - 2D – NACA 64-012 solution: a) $M\infty=0.73$; b) Peak underpressure of the $M\infty=0.73$ solution.

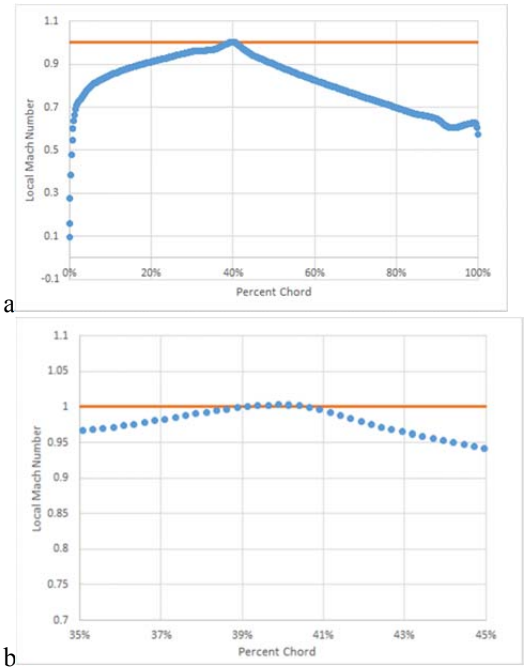

Figure 21. ANSYS/Fluent local Mach number over the NACA 64-012 airfoil: a) Mach number over the entire airfoil, b) Mach number at the location of the peak underpressure.

(Figure 20), Eastman Jacobs, Anderson, and Küchemann all correctly predict the critical condition.

In order to verify the data from the CFD computations, we performed a grid density study. We performed this study by refining the grid step size by a factor of 1.5 two times over, in turn giving three total grids. From these grids the M∞=0.725 solution was run and the minimum pressure coefficient, and the Mach number at this location, was compared across each of the grids. Table 1 shows the results of the grid refinement.

Table 1 shows confidence in the current calculations. The grid convergence shows that although the observed order is less than the order of the method, the data gathered is converging and the errors decreasing. Therefore, the current data is computed on a grid that has a sufficiently small step size.

Table 1. CFD Validation Case Data.

Step Size (h)	**Minimum Pressure (Cp_{min})**	**Maximum Mach**
1	-0.67989	0.9937
1.5	-0.67863	0.9905
2.25	-0.67606	0.9848
Richardson Extrapolation	-0.6811	0.9982
Observed Order (p)	1.766	1.352
GCI_{12} (Error band)	0.221%	0.559%
GCI_{23} (Error band)	0.453%	0.970%
Asymptote	0.99815	0.9967

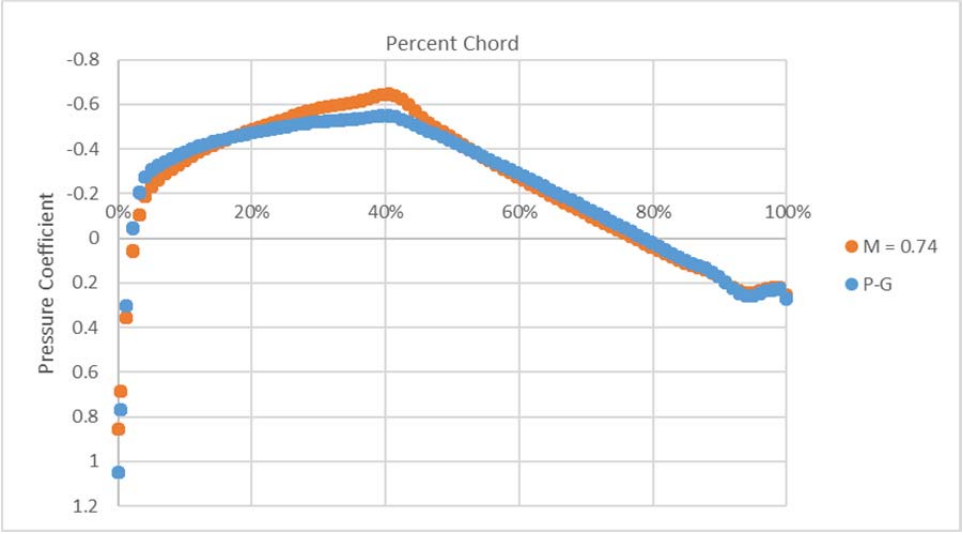

Figure 22 – ANSYS/FLUENT computation – 2D – NACA 64-012 solution. Comparison of high-speed vs P-G corrected low-speed data.

Figure 22 demonstrates the utility and limitations of the simple Prandtl-Glauert transformation. We compare the low-speed, but Prandtl-Glauert corrected data (using Equation 11) against to the M∞=0.74 compressible flow solution from ANSYS. We can see how for high-speed, yet subcritical flow, Prandtl's transformation on the low speed flow is approximate, but reasonably good. We also see a wider discrepancy around the location of peak underpressure, where local supersonic flow exists; and near the leading edge of the airfoil where Prandtl himself warned of the limitations of the correction. In these locations the approximation is poor.

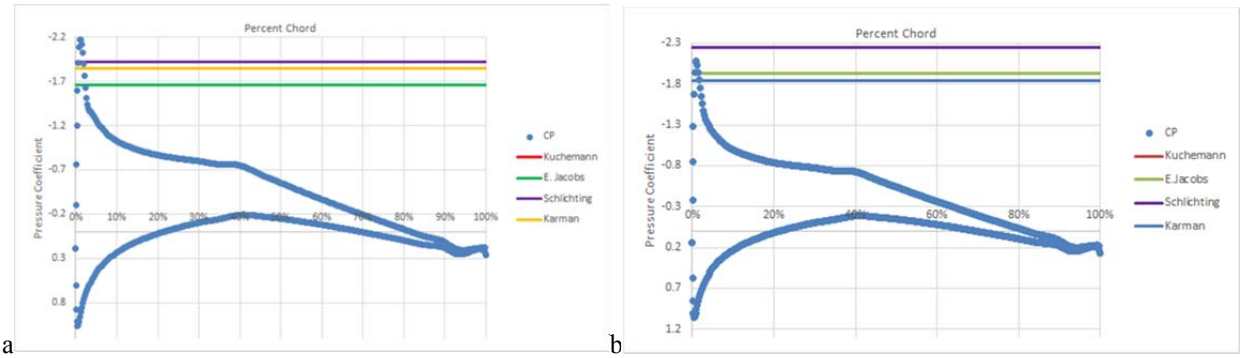

a b

Figure 23 – ANSYS/FLUENT computation – 2D – NACA 64-012 solution four degrees angle of attack: a) M∞=0.55; b) M∞=0.52

The next testing was done on the NACA 64-012 airfoil at four degrees angle of attack. The data here shows that at M∞ = 0.55 a shock wave has formed near the leading edge of the airfoil, which is correctly predicted by each author. Figure 23a shows the pressure coefficient over the airfoil and shows that the Eastman Jacobs, Küchemann, Anderson, Schlichting, and Von Kármán are indeed correct in predicting this shock wave. However, in order to determine who predicts the critical point, we lowered the freestream Mach number to find the point in which the shock wave begins to form.

Figure 23b shows the pressure coefficient for M∞=0.52. The data here shows a peak in the pressure coefficient near the leading edge, and a shock wave is in the early stages of forming. A check on the local Mach number does indeed indicate that the critical condition has been met on the airfoil. We found that Eastman Jacobs, Küchemann, Anderson, and Schlichting correctly predict this condition.

From the data presented, we concluded that Eastman Jacobs, Küchemann, and Anderson are all correct in their derivation of the critical pressure coefficient for the two-dimensional unswept section. These three authors derived their results based upon thermodynamic relationships. Therefore, for an inviscid solution it makes sense that these three authors had the correct derivation for the Critical Pressure Coefficient.

V. CONCLUSIONS

As a first step in documenting the best formula to estimate the Critical Mach Number of a wing from a potential flow solution, we revisited the Transonic Similarity Rule. Close reading of the primary and secondary source literature revealed a multitude of differing interpretations and explanations of the physical transformation implied by the foundational mathematics. The famous authors[5,6,7,8,9,10,11,12,13] all state that there is a geometrical transformation, causing a change in the wing area, aspect ratio, thickness and incidence. Some authors[5,12] hand wave through the explanation to state there is only a difference in the results. These conflicting explanations do not give insight into the actual "stretching" that is applied to the compressible flow. Through the use of *VORLAX*, CFD (*ANSYS FLUENT*), and some *JAVAFOIL* solutions, we found that the geometrical "stretching" explanation does not properly describe code results.

Schlichting[5] summarized the Prandtl-Glauert transformations as part of his Transonic Similarity Rule. He provided a table of all of the transformations that should occur, including geometric "stretching". In the work of this paper, we found Schlichting to have the correct transformation for the pressure distribution, the lift curve slope, zero lift angle, and the lift coefficient. These correlations imply that the "stretching" is not geometric, but instead a Mach dependent velocity "scaling" applied to the actual geometry (see the geometrical analogy described by Figure 1C).

Schlichting's transformation of the coefficient of pitching moment and the induced drag does not match our compressible solution. The pitching moment transformation cannot follow the Prandtl-Glauert transformation due to the coupling of the lift transformation, as well as a Mach transformation on the aerodynamic center. The transformation on the induced drag is defined by Schlichting as the transformation on the lift as well as the

transformation on the Aspect Ratio. This transformation is defined by a velocity "stretching" in the lift coefficient, and a geometric transformation through the decrease in the Aspect Ratio. Figure 17 shows that this transformation is not correct. Instead the current authors find that drag due to lift scales with the square of the high speed lift coefficient: an effective scaling transformation factor of a $\frac{1}{1-M_\infty^2}$ as opposed to Schlichting's $\frac{1}{\sqrt{1-M_\infty^2}}$ relationship.

Our evidence shows that most of the manifestations of the Prandtl-Glauert rule that have previously been explained by some sort of "stretching" can be better explained by a velocity "scaling" analogy. Data presented here paper shows that various proposed transformations of high speed geometry into an altered, equivalent incompressible solution geometry introduce an effective angle of attack change, area change or aspect ratio change that has been contradicted by the computational results of accepted codes.

We also found many different published equations that purport to estimate the Critical Mach and Critical Pressure Coefficient, and hence predict the onset of sonic flow. Here, we have shown that these equations vary significantly in the range of which real transonic aircraft experience incipient shock-wave formation.

Using *ANSYS Fluent* to solve the Navier-Stokes equations, we set forth to determine which equation is correct in estimating the Critical Pressure Coefficient. By comparing the minimum pressure and the local Mach number on the airfoil, we found that the thermodynamic derivations of Eastman Jacobs, Küchemann, and Anderson correctly predicts the sonic point on the airfoil.

Acknowledgements

Mr. Kirkman performed this unsponsored research activity in partial fulfillment of the degree requirements for obtaining his M.S. in Aerospace Engineering from Arizona State University.

References

[1] Takahashi, T.T., Dulin, D.J. and Kady, C.T., "A Method to Allocate Camber, Thickness and Incidence on a Swept Wing," AIAA 2014-3172, 2014

[2] Busemann, A. "Aerodynamischer Auftrieb bei Ubershallgeschwindigkeit," Luftfahrtforschung Vol. 12, No. 6, 1935, pp. 210-215.

[3] Meier, H.-U. Editor, German Development of the Swept Wing 1935-1945, AIAA, 2010 (Contains a formal English language translation of Busemann, A. "Aerodynamischer Auftrieb bei Ubershallgeschwindigkeit," found in G.A. Crocco, (ed) "Convego di Scienze Fisiche, Matematiche e Naturali," Tema: Le Alta Velocitia in Aviazione, Reale Accademia d'Italia, Fondazione Alessandro Volta, Sept. 30-Oct. 6, 1935, Rome, Italy, p. 328-360 (1935).)

[4] Takahashi, T.T. and Kamat, S., "Revisiting Busemann: The Design Implications of Inconsistencies Found Within Simple Sweep Theory," AIAA 2015-3376, 2015.

[5] Schlichting. J. and Truckenbrodt, E. *Aerodynamics of the Airplane*, McGraw-Hill, 1979

[6] Küchemann, D., *The Aerodynamic Design of Aircraft*, AIAA, 2012.

[7] Von Kármán, Th., "Compressibility Effects in Aerodynamics," J. of the Aeronautical Sciences, Vol. 8, No. 9, 1941, p. 337

[8] Prandtl, L., "General Considerations on the Flow of Compressible Fluids," NACA TM-805, 1936 (A formal English translation of Prandtl, L. "Allgemine Überlegungen über die Strömung zusammaendrückbarer Flüssigkeiten." Convego di Scienze Fisiche, Matematiche e Naturali," Tema: Le Alta Velocitia in Aviazione, Reale Accademia d'Italia, Fondazione Alessandro Volta, Sept. 30-Oct. 6, 1935, Rome, Italy

[9] Göthert, B., "Plane and Three Dimensional Flow at High Speeds," NACA TM-1105, 1946. (A formal English translation of: Göthert, B.," Ebene und ramliche Stromung bie hohen Unterschallgeschwindigkeiten," Lillienthal Gesellschaft 127.)

[10] Jones, R.T., "Wing Planforms for High Speed Flight," NACA TR-863, 1947.

[11] Jones, R.T. and Cohen, D. *High Speed Wing Theory*, Princeton University Press, 1960.
[12] McLean, D., *Understanding Aerodynamics: Arguing from the Real Physics*, Wiley, 2012.
[13] Drela, M., *Flight Vehicle Aerodynamics*, MIT Press, 2014.
[14] Glauert, H., "The Effect of Compressibility on the Lift of Airfoils," Proc. Of the Royal Society of London (Series A), Vol 118, p. 113, 1927.
[15] Abbott, I.A., von Doehnhoff, A.E. and Stivers, L.S., "Summary of Airfoil Data," NACA TR-824, 1945.
[16] Anderson, J.D. *Introduction to Flight*, 5th Edition, McGraw-Hill, 2005.
[17] Miranda, L. R., Baker, R. D., and Elliott, W. M., "A Generalized Vortex Lattice Method for Subsonic and Supersonic Flow," NASA CR 2875, 1977.
[18] *See:* http://www.mh-aerotools.de/airfoils/*JAVAFOIL*.htm (accessed Oct 29, 2015).
[19] SAS IP, Inc., "Section 20.1.2. Density-Based Solver", The ANSYS Fluent Getting Started Guide, Release 15.0
[20] Harris, C.D., "Two Dimensional Aerodynamic Characteristics of the NACA 0012 Airfoil in the Langley 8-foot Transonic Pressure Tunnel," NASA TM 81927, 1981.